INFN/AE - 67/10
30 Settembre 1967

ANTIPROTON - PROTON ELASTIC SCATTERING BETWEEN 63 and 175 MeV

B. Conforto, G. Fidecaro and H. Steiner (*)
CERN - Geneva

R. Bizzarri, P. Guidoni and F. Marcelja
Istituto di Fisica dell'Università - R o m a
Istituto Nazionale di Fisica Nucleare - Sezione di Roma

G. Brautti, E. Castelli, M. Ceschia and M. Sessa
Istituto di Fisica dell'Università - T r i e s t e
Istituto Nazionale di Fisica Nucleare - Sezione di Trieste

(*) J.S. Guggenheim Fellow. Permanent address:
University of California, Berkeley, California.

SUMMARY

The $\bar{p}p$ elastic scattering differential cross-sections have been determined at nine energies between 63 and 175 MeV, from 11000 scattering events measured in a Hydrogen Bubble Chamber. The results are compared with existing theoretical models and good agreement is found with the calculations of Bryan and Phillips.

SOMMARIO

Sono state determinate le sezioni d'urto differenziali elastiche $\bar{p}p$ a nove energie tra 63 e 175 MeV, da 11000 eventi in camera a bolle a idrogeno. Si fa il confronto dei risultati ottenuti con gli esistenti modelli teorici, trovando un buon accordo con i calcoli di Bryan e Phillips.

INTRODUCTION

This work is part of a study on antiproton interactions in hydrogen at low energies, using the bubble chamber technique.

The behaviour of annihilation, total elastic and total zero-prongs cross-sections has been the object of a previous paper (1), henceforth referred to as I. Here we present the results on the elastic-scattering differential cross-section.

These distributions have already been measured by Coombes et al. (2) down to 133 MeV using counter detectors, by Cork et al. (3) from 45 to 245 MeV using hydrogen bubble chamber and by Hossain and Shaukat (4) from 5 to 60 MeV using nuclear emulsions. In order to achieve a higher energy resolution and a better statistical accuracy we have analyzed 42,000 pictures taken from the 81 cm Saclay Hydrogen Bubble Chamber exposed to a separated beam of antiprotons from the CERN PS. From these we obtained 11,000 events, divided in 9 energy intervals from 63 to 175 MeV, and the corresponding angular distributions were computed. These distributions, when fitted with Legendre polynomials, show the contribution of angular momenta up to (at least) L = 2 below 100 MeV kinetic energy, and (at least) L = 3 above that limit. The distributions of the same events as a function of the four-momentum transfer show a slope corresponding to an "effective radius" decreasing with energy, according to $R_{eff} = R_o + \lambda\!\!\!^{-}$ (R_o is about 1 Fermi, and $\lambda\!\!\!^{-}$ is the wave length of the relative motion in $p\text{-}\bar{p}$ center of mass).

Several simplified theoretical models have attempted to describe the non-relativistic $\bar{p}p$ interaction. Our data show a very good agreement with results from a calculation by Bryan and Phillips (13).

A preliminary account of this experiment has already been published (5).

1. - EXPERIMENTAL PROCEDURE

The pictures used for this experiment were obtained exposing the 81 cm Saclay HBC to a separated beam of low energy antiprotons at the CERN PS (6).

Three exposures of the HBC have been made, covering the energy interval from 50 to 190 MeV. The exposure conditions, and the determination of the beam energies at the entrance in the bubble chamber (125, 156 and 190 MeV) have been described in I.

42,000 pictures were scanned for elastic antiproton interaction. The elastic events are easily recognized (vs two prong annihilations) at the scanning table, due to the heavy ionization of both the outgoing prongs. The π^- contamination of the beam was negligible, (<0.1%) as discussed in I.

The events were measured by projecting the film at about life size magnification on digitized tables with a typical measuring error of 0.1 mm. The measurements were processed through the chain of CERN programs THRESH, GRIND, CULL, SUMX.

Since very backward scatterings have a higher failure rate due to the short track length of the scattered antiproton, to avoid biases all the events that failed in geometry

or kinematics have been remeasured. About 1% of the events still failed after the third measurement. These events did not show any appreciable bias. For each of them the center-of-mass scattering angle has been computed by hand from the available geometrical informations.

The incoming antiprotons have been accepted for further analysis only if they entred the chamber within a predetermined "beam window", and within a small cone around the average beam direction. The determination of the acceptance criteria has been fully described in I.

The events collected from each exposure have been further divided into three groups, according to the path length of the incident antiproton. In Table I we give the average incident energy for each of the nine groups, as determined from the known beam energy taking into account the energy lost in the hydrogen. The values agree with those obtained from the kinematic fit.

TABLE I

Laboratory kinetic energy (MeV)	Total cross-section σ_t (mb)	Total elastic cross-section σ_s (mb)	$[\mathrm{Im}\ f(0)]^2$ (mb/sr)	Number of events ($\cos\vartheta^* \leq 0.970$)
62.7 ± 13.3	224.5 ± 6.6	77.6 ± 3.3	24.17 ± 1.42	1281
83.5 ± 10.5	199.7 ± 5.5	71.1 ± 2.8	25.45 ± 1.40	1364
99.8 ± 9.1	188.0 ± 4.9	68.7 ± 2.5	27.00 ± 1.41	1465
110.0 ± 8.4	179.5 ± 4.5	62.0 ± 2.2	27.12 ± 1.36	1522
124.3 ± 7.0	171.1 ± 4.5	62.6 ± 2.3	27.86 ± 1.47	1186
136.8 ± 6.5	169.2 ± 4.1	59.5 ± 2.1	29.98 ± 1.45	1240
150.9 ± 6.7	167.6 ± 3.5	63.5 ± 2.2	32.46 ± 1.36	904
163.3 ± 6.3	161.1 ± 3.2	61.3 ± 2.0	32.44 ± 1.29	974
175.0 ± 6.0	154.3 ± 3.0	57.3 ± 1.8	31.90 ± 1.24	1038
				Total 10974

To obtain the energy distribution of the events in each interval, the residual range distribution of the beam (very nearly a gaussian, see I) was folded in. The resulting distribution is shown in Fig. 1. From the range spread ΔR, calculated as half width at half heigth of the curve, we compute the energy spread ΔE as given Table I. In this way 80% of the events are contained in the interval $\pm\Delta E$ around E.

In Table I we also report, for each energy interval, the values of the total (σ_t) and the elastic (σ_s) cross-section as determined from the data obtained in I. From the value

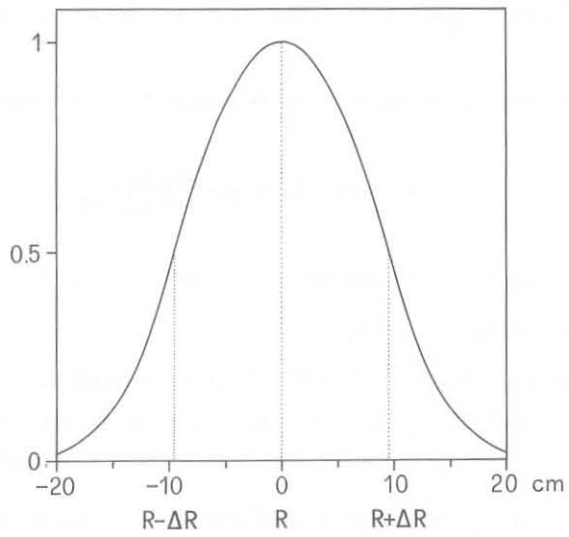

Fig. 1 - Distribution of residual range around the central value for each energy interval.

of σ_t, the square of the imaginary part of the forward scattering amplitude has been computed by the use of the optical theorem. In the last column of Table I the number of measured elastic scattering events that satisfy our selection criteria is given for each energy interval.

2. - DIFFERENTIAL CROSS-SECTIONS

The cosine of the center-of-mass scattering angle $\cos \vartheta^*$ has been computed for each measured event.

To avoid large and uncertain efficiency corrections, all the events found in scanning have been measured but only those with a laboratory scattering angle large than 7° ($\cos\vartheta^* \leq 0.97$) have been retained, since the detection probability of an event decreases rapidly with decreasing scattering angle.

The events within each energy interval have been divided into 40 bins according to the value of $\cos\vartheta^*$. Each bin corresponds then to an interval $\Delta\cos\vartheta^* = 0.05$, except the last one, for which $\Delta\cos\vartheta^* = 0.97 - 0.95 = 0.02$.

For the events in each bin the distribution of the normal to the scattering plane about the direction of the incoming track has been examined. In the last 4 bins some losses of events with a scattering plane almost normal to the bubble chamber windows are apparent. This loss has been corrected by requiring the above mentioned distributions to be uniform. The resulting correction amounts to about 3% of the total of the events. Finally in each bin the contribution of Coulomb scattering has also been subtracted. No attempt to take

into account the possible contribution of interference between Coulomb and nuclear scattering has been made.

The differential scattering cross-section has then been computed as

$$\frac{d\sigma}{d\Omega}(\cos\vartheta^*_i) = \frac{n_i\,\sigma'_s}{2\pi N \Delta \cos\vartheta^*_i}$$

where n_i = corrected number of events in the interval $\Delta\cos\vartheta^*_i$ around $\cos\vartheta^*_i$

N = number of events = $\sum_1^{40} i\ n_i$

σ'_s = the integral of the $\frac{d\sigma}{d\Omega}(\cos\vartheta^*)$ between -1 and 0.97 as determined in I. (We recall that is σ'_s the experimentally accessible quantity, while the total elastic cross-section σ_s has been obtained through an extrapolation).

The resulting values of $\frac{d\sigma}{d\Omega}$ with their statistical errors are given in Table II and displayed in Fig. 2. On the same figure the Coulomb contribution which has been substracted from the raw data is shown as a full line; the solid dot represents the minimum forward cross-section predicted by the optical theorem. The shaded areas represent the contribution of the corrections for the events lost due to the orientation of the scattering plane. These angular distributions are in good agreement with the ones obtained by previous experiments in the same energy range ([2,3]) with smaller statistics.

For each event the square of the four momentum transfer t has also been computed and $d\sigma/dt$ has been evaluated in a way completely analogous to $d\sigma/d\Omega$. The cut at small scattering angles ($\cos\vartheta^* \leq 0.97$) corresponds to a cut in the low momentum transfer which varies with the incident energy from -0.002 to -0.004 $(GeV/c)^2$. The results for $d\sigma/dt$ are shown in the 9 histograms of Fig. 3 for $|t| \leq 0.2\ (GeV/c)^2$. For typographical reasons in the last 6 histograms respectively 3, 20, 23, 17, 20, 28 events with $|t| > 0.2\ (GeV/c)^2$ are not shown.

3. - DISCUSSION OF RESULTS

At each energy the angular distribution has been fitted using a maximum likelihood procedure to a Legendre polynomial expansion

$$\frac{d\sigma}{d\Omega}(\cos\vartheta^*) = \sum_0^{2L} a_n P_n(\cos\vartheta^*)$$

The optical point has been introduced with its error as an indipendent lower limit to the forward cross-section.

Resulting curves for the case L = 3 are shown in Fig. 2 (dashed lines). They give a good fit at all the energies and no contribution of L = 4 is required. For the three lowest energies (below 100 MeV) a satisfactory fit is obtained also with L = 2. Above 100 MeV however L = 3 is necessary (*).

(*) From a comparison of the elastic to the total $\bar{p}p$ cross-sections, in I was shown that incident waves with angular momentum up to 2 must contribute to the annihilation.

TABLE II

Laboratory kinetic energy (MeV)	CENTER-OF-MASS DIFFERENTIAL CROSS-SECTIONS (mb/sr)								
	62.7	83.4	99.8	110.0	124.3	136.8	150.9	163.3	175.0
cos ϑ^*									
-0.975	0.4 ± 0.3	0.2 ± 0.2	0.8 ± 0.3	0.5 ± 0.2	0.9 ± 0.4	0.7 ± 0.3	0.2 ± 0.2	0.2 ± 0.2	0.5 ± 0.3
-0.925	0.0 ± 0.0	0.0 ± 0.0	0.3 ± 0.2	0.1 ± 0.1	0.8 ± 0.3	0.8 ± 0.3	1.0 ± 0.4	0.2 ± 0.2	0.5 ± 0.3
-0.875	0.2 ± 0.2	0.2 ± 0.2	0.1 ± 0.1	0.2 ± 0.2	0.8 ± 0.3	0.6 ± 0.3	0.6 ± 0.3	0.4 ± 0.3	0.8 ± 0.4
-0.825	0.0 ± 0.0	0.2 ± 0.2	0.1 ± 0.1	0.5 ± 0.2	0.6 ± 0.3	0.3 ± 0.2	0.4 ± 0.3	0.4 ± 0.3	0.2 ± 0.2
-0.775	0.7 ± 0.4	0.3 ± 0.2	0.6 ± 0.3	0.5 ± 0.2	0.6 ± 0.3	0.7 ± 0.3	0.2 ± 0.2	0.2 ± 0.2	0.2 ± 0.2
-0.725	0.2 ± 0.2	0.3 ± 0.2	0.3 ± 0.2	0.1 ± 0.1	0.0 ± 0.0	0.6 ± 0.3	0.4 ± 0.3	0.2 ± 0.2	0.5 ± 0.3
-0.675	0.7 ± 0.4	0.2 ± 0.2	0.3 ± 0.2	0.0 ± 0.0	0.2 ± 0.2	0.0 ± 0.0	0.2 ± 0.2	0.4 ± 0.3	0.3 ± 0.2
-0.625	1.1 ± 0.4	0.2 ± 0.2	0.0 ± 0.0	0.1 ± 0.1	0.2 ± 0.2	0.1 ± 0.1	0.2 ± 0.2	0.7 ± 0.4	0.3 ± 0.2
-0.575	0.9 ± 0.4	0.0 ± 0.0	0.3 ± 0.2	0.1 ± 0.1	0.3 ± 0.2	0.0 ± 0.0	0.2 ± 0.2	0.2 ± 0.2	0.3 ± 0.2
-0.525	0.2 ± 0.2	0.2 ± 0.2	0.0 ± 0.0	0.1 ± 0.1	0.0 ± 0.0	0.1 ± 0.1	0.0 ± 0.0	0.0 ± 0.0	0.3 ± 0.2
-0.475	1.1 ± 0.4	0.2 ± 0.2	0.6 ± 0.3	0.1 ± 0.1	0.2 ± 0.2	0.0 ± 0.0	0.0 ± 0.0	0.0 ± 0.0	0.3 ± 0.2
-0.425	0.9 ± 0.4	0.6 ± 0.3	0.4 ± 0.2	0.2 ± 0.2	0.5 ± 0.3	0.3 ± 0.2	0.0 ± 0.0	0.7 ± 0.4	0.0 ± 0.0
-0.375	1.1 ± 0.4	0.8 ± 0.3	0.4 ± 0.2	0.2 ± 0.2	0.2 ± 0.2	0.4 ± 0.2	0.0 ± 0.0	0.0 ± 0.0	0.0 ± 0.0
-0.325	1.4 ± 0.5	0.8 ± 0.3	1.0 ± 0.4	0.2 ± 0.2	0.0 ± 0.0	0.1 ± 0.1	0.2 ± 0.2	0.2 ± 0.2	0.3 ± 0.2
-0.275	1.6 ± 0.5	0.9 ± 0.4	0.7 ± 0.3	0.6 ± 0.3	0.3 ± 0.2	0.1 ± 0.1	0.0 ± 0.0	0.2 ± 0.2	0.0 ± 0.0
-0.225	1.6 ± 0.5	1.1 ± 0.4	1.0 ± 0.4	0.8 ± 0.3	0.5 ± 0.3	0.4 ± 0.2	0.2 ± 0.2	0.2 ± 0.2	0.0 ± 0.0
-0.175	3.2 ± 0.8	1.4 ± 0.5	1.2 ± 0.4	0.7 ± 0.3	0.2 ± 0.2	0.0 ± 0.0	0.8 ± 0.4	0.4 ± 0.3	0.0 ± 0.0
-0.125	4.5 ± 0.9	1.7 ± 0.5	1.4 ± 0.4	0.7 ± 0.3	0.6 ± 0.3	0.7 ± 0.3	0.0 ± 0.0	0.4 ± 0.3	0.0 ± 0.0
-0.075	2.1 ± 0.6	3.5 ± 0.7	1.2 ± 0.4	1.4 ± 0.4	1.5 ± 0.5	0.7 ± 0.3	0.2 ± 0.2	0.0 ± 0.0	0.0 ± 0.0
-0.025	2.7 ± 0.7	1.5 ± 0.5	1.9 ± 0.5	1.8 ± 0.5	1.4 ± 0.5	1.3 ± 0.4	0.2 ± 0.2	0.2 ± 0.2	0.5 ± 0.3
0.025	4.5 ± 0.9	1.8 ± 0.5	1.9 ± 0.5	1.5 ± 0.4	0.9 ± 0.4	1.4 ± 0.4	0.6 ± 0.3	1.1 ± 0.4	0.5 ± 0.3
0.075	4.1 ± 0.9	2.9 ± 0.7	2.1 ± 0.5	2.1 ± 0.5	1.5 ± 0.5	2.4 ± 0.6	0.4 ± 0.3	1.3 ± 0.5	0.8 ± 0.4
0.125	6.1 ± 1.0	5.1 ± 0.9	3.6 ± 0.7	3.0 ± 0.6	2.2 ± 0.6	1.5 ± 0.5	1.2 ± 0.5	1.3 ± 0.5	0.6 ± 0.3
0.175	3.6 ± 0.8	4.8 ± 0.9	1.8 ± 0.5	3.4 ± 0.6	3.1 ± 0.7	2.0 ± 0.5	1.8 ± 0.6	1.8 ± 0.6	1.4 ± 0.5
0.225	6.1 ± 1.0	4.2 ± 0.8	5.0 ± 0.8	3.8 ± 0.7	2.3 ± 0.6	2.5 ± 0.6	2.2 ± 0.7	0.9 ± 0.4	1.6 ± 0.5
0.275	7.7 ± 1.2	5.4 ± 0.9	4.0 ± 0.7	4.5 ± 0.7	4.9 ± 0.9	3.6 ± 0.7	3.2 ± 0.8	2.5 ± 0,7	1.6 ± 0.5
0.325	7.7 ± 1.2	4.2 ± 0.8	6.0 ± 0.9	4.9 ± 0.8	5.1 ± 0.9	2.4 ± 0.6	3.4 ± 0.8	3.1 ± 0.7	2.8 ± 0.7
0.375	7.1 ± 1.1	8.8 ± 1.2	6.1 ± 0.9	5.9 ± 0.8	6.9 ± 1.0	4.6 ± 0.8	3.8 ± 0.9	2.7 ± 0.7	3.2 ± 0.7
0.425	11.1 ± 1.4	6.9 ± 1.0	6.4 ± 0.9	6.5 ± 0.9	6.0 ± 1.0	7.0 ± 1.0	4.6 ± 1.0	4.1 ± 0.9	3.0 ± 0.7
0.475	8.4 ± 1.2	8.6 ± 1.2	8.7 ± 1.1	6.8 ± 0.9	7.1 ± 1.0	6.7 ± 1.0	5.8 ± 1.0	6.7 ± 1.1	4.7 ± 0.9
0.525	9.8 ± 1.3	11.5 ± 1.3	10.7 ± 1.2	8.7 ± 1.0	7.5 ± 1.1	6.0 ± 0.9	8.2 ± 1.3	6.8 ± 1.1	5.8 ± 1.0
0.575	11.1 ± 1.4	9.7 ± 1.2	10.9 ± 1.2	8.0 ± 1.0	9.1 ± 1.2	8.8 ± 1.1	8.6 ± 1.3	7.4 ± 1.2	7.3 ± 1.1
0.625	13.6 ± 1.6	10.9 ± 1.3	13.8 ± 1.4	8.9 ± 1.0	9.4 ± 1.2	8.5 ± 1.1	8.8 ± 1.3	8.7 ± 1.2	9.5 ± 1.2
0.675	15.3 ± 1.7	11.7 ± 1.3	11.5 ± 1.3	14.0 ± 1.3	11.7 ± 1.3	11.2 ± 1.3	10.9 ± 1.5	12.1 ± 1.5	10.1 ± 1.3
0.725	15.7 ± 1.7	12.6 ± 1.4	13.3 ± 1.4	10.6 ± 1.1	12.3 ± 1.4	13.3 ± 1.4	14.9 ± 1.7	10.6 ± 1.4	14.0 ± 1.5
0.775	16.0 ± 1.7	17.8 ± 1.7	15.1 ± 1.4	14.1 ± 1.3	13.8 ± 1.5	14.4 ± 1.4	18.1 ± 1.9	16.4 ± 1.7	12.3 ± 1.4
0.825	14.7 ± 1.6	18.4 ± 1.7	20.2 ± 1.7	15.5 ± 1.4	16.7 ± 1.6	15.9 ± 1.5	20.5 ± 2.0	19.6 ± 1.9	18.6 ± 1.7
0.875	17.0 ± 1.7	20.4 ± 1.8	21.8 ± 1.7	19.0 ± 1.5	18.8 ± 1.7	22.3 ± 1.8	25.1 ± 2.2	24.8 ± 2.1	23.0 ± 1.9
0.925	18.1 ± 1.8	20.5 ± 1.8	18.6 ± 1.6	20.5 ± 1.6	24.8 ± 2.0	21.6 ± 1.7	20.9 ± 2.1	27.6 ± 2.2	27.0 ± 2.1
0.960	18.0 ± 2.8	25.0 ± 3.1	22.9 ± 2.8	25.0 ± 2.7	22.2 ± 2.9	23.4 ± 2.9	36.1 ± 4.3	28.3 ± 3.6	28.0 ± 3.3
Optical point	24.2 ± 1.4	25.5 ± 1.4	27.0 ± 1.4	27.1 ± 1.4	27.9 ± 1.5	30.0 ± 1.5	32.5 ± 1.4	32.4 ± 1.3	31.9 ± 1.2

The distribution in t show a diffraction-like behaviour, the width of the diffraction peak increasing with the antiproton energy.

The distribution of the diffraction scattering from a black sphere of radius R can be expressed in the form

$$\frac{d\sigma}{dt} = \pi R^2 \frac{J_1^2\left(\frac{R}{\hbar}\sqrt{|t|}\right)}{|t|}$$

provided the wave length λ of the relative motion of the colliding particles is small compared to the radius R. This is not the case in this experiment, λ ranging from 1.15 to 0.7 fm. We have however attempted to fit the forward part of $d\sigma/dt$, for $-t < 0.05$ $(GeV/c)^2$, with an expression of the type

$$(1) \qquad \frac{d\sigma}{dt} = A_i \frac{J_1^2\left(\frac{R_i}{\hbar}\sqrt{|t|}\right)}{|t|}$$

A_i and R_i being free parameters to be determined for each of the 9 values of the incident energy E_i. The result of the fit is very satisfactory, the probability associated with the overall χ^2 being 30%. Of course the agreement is limited to the small momentum transfers, the experimental data presenting a tail of high momentum transfer events not reproduced by formula (1).

The values of the diffraction radii R_i decrease with increasing energy corrisponding to the increase in the width of the peak. This variation of R with energy can be well represented by $R_i = a + \lambda_i$. In fact a fit to the expression

$$(2) \qquad \frac{d\sigma}{dt} = A_i \frac{J_1^2\left[\left(\frac{a+\lambda}{\hbar}\right)\sqrt{|t|}\right]}{|t|}$$

with $\underline{a}$ independent of the incident energy, gives an equally satisfactory result, the associated χ^2 probability being again 30%. The value of $\underline{a}$ is $\underline{a} = 1.03$ fm, in reasonable agreement with the value a = 0.90 fm obtained in I by fitting the annihilation cross-section to the form $\sigma_a = \pi\ (a+\lambda)^2$.

No clear energy dependence of the coefficients A_i is apparent. However a simple fit to the 9 distributions according to the form

$$(3) \qquad \frac{d\sigma}{dt} = (b+c\lambda) \frac{J_1^2\left[\left(\frac{a+\lambda}{\hbar}\right)\sqrt{|t|}\right]}{|t|}$$

gives a reasonable fit ($P(\chi^2) = 4\%$) with the following values for the parameters

$$a = 1.04 \text{ fm}$$
$$b = 29.4 \text{ mb}$$
$$c = 49.5 \text{ mb fm}^{-1}$$

if λ is expressed in fm and then $\hbar = 0.197 \frac{GeV \cdot fm}{c}$.

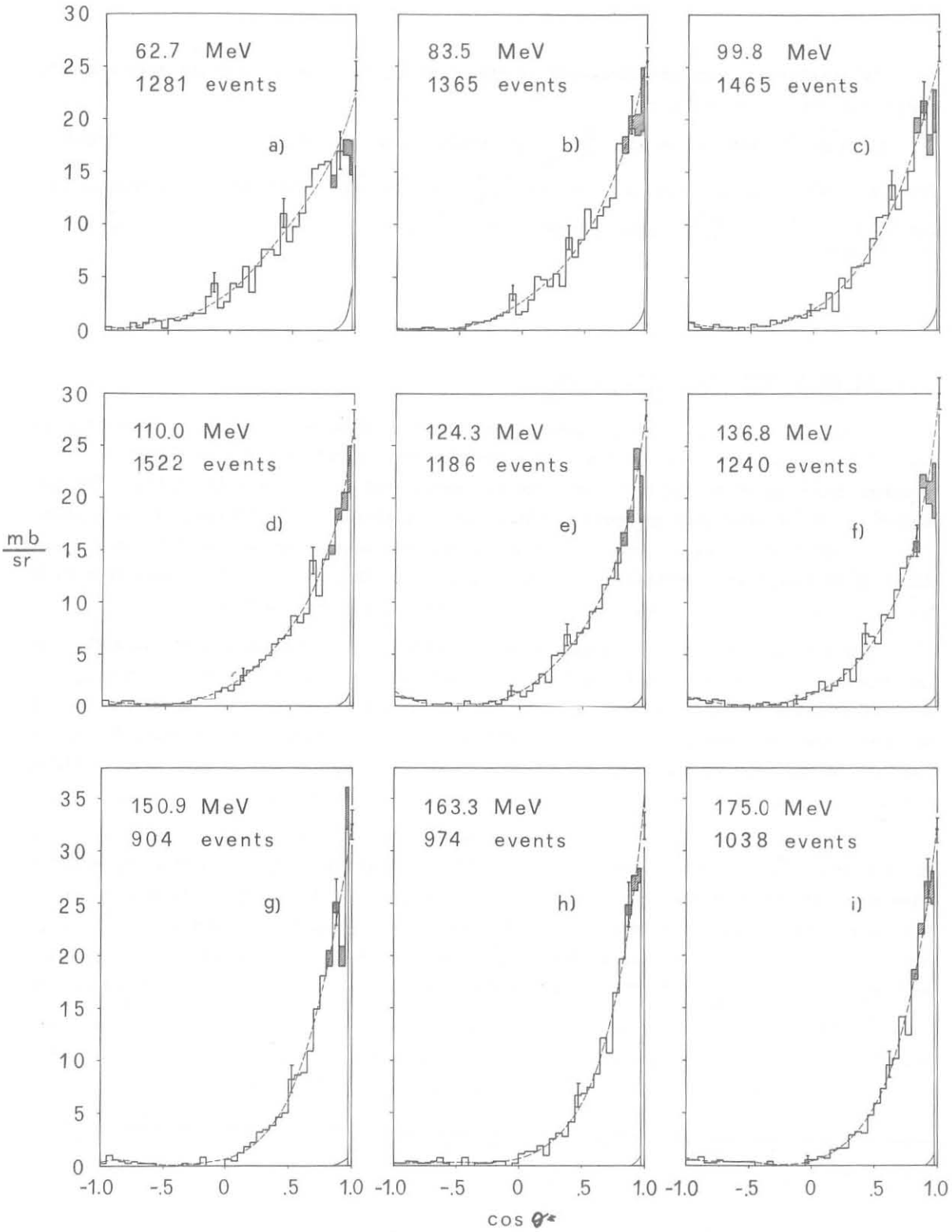

Fig. 2 - Center-of-mass differential cross-sections $d\sigma/d\Omega$ for the 9 energy values. The full line is the Coulomb differential cross-section which has been subtracted. The solid dot represents the optical point, and the shaded areas the correction due to scattering plane orientation. The dashed line is the fit with Legendre polynomial for L = 3. Typical errors are shown.

The resulting curves are desplayed in Fig. 3 as dashed lines. They are very close to those from the 10 parameters fit.

In Table III the values of $\left(\frac{d\sigma}{dt}\right)_{t=0}$ as obtained from the optical point are compared, for the 9 values of λ, with the values $\left(\frac{d\sigma}{dt}\right)_{t=0} = \frac{A_i}{4}\frac{(a+\lambda)^2}{\hbar^2}$ obtained from formula (2) and $\left(\frac{d\sigma}{dt}\right)_{t=0} = \frac{(b+c\lambda)}{4}\frac{(a+\lambda)^2}{\hbar^2}$ obtained from formula (3).

4. - COMPARISON WITH THEORETICAL MODELS

In the low (non relativistic) energy range, the $N\bar{N}$ interaction can be treated by a potential whose real part can, at least in principle, be deduced from the NN potential by changing the sign of the contributions due to exchange of an odd G parity sistem. The contribution of the annihilation process (which has no analogue in the NN case) in then added in a phenomenological way either by introducing a completely absorptive central core or by means of an imaginary potential. A comparison of the different existing calculations with the measured total elastic and inelastic cross-sections has been done in I.

In comparing the predicted shapes of differential scattering cross-sections with the experimental results, if must be kept in mind that the bulk of the elastic scatterings is contained in the forward diffraction peak. As a consequence any theoretical model capable of predicting the total elastic and inelastic cross-sections will reproduce also the gross features of the angular distributions. Predictions of different models will however differ when considering finer details, for example the amount of backward scattering.

The first quantitative attempt to describe the $N\bar{N}$ interaction along these lines is due to Ball and Chew ([7]). They represent the annihilation interaction by a completely absorptive core, and using WKB approximation they compute cross-sections which are independent of the core radius. This model has been applied by Fulco ([8]) and by Ball and Fulco ([9]) to calculate the elastic angular distribution. The results are in only qualitative agreement with experiment, the main difficulty being that the elastic cross-section is overestimated.

The same model has been used by Ceschia and Perlmutter ([10]), who however avoided the use of WKB approximation and explicitely solved the Schroedinger equation by introducing a boundary condition of the type e^{-iKr} at a certain value r = R of the radius. The two parameters R and K/k (k = wave number of the incident wave) are fitted to the experimental data. In I it was shown that a fair agreement with the measured cross-sections was obtained in this way with the choice $R = \frac{2}{3}\lambda_\pi$, K/k = 1/2. The corresponding angular distributions are compared with the data in Fig. 4.b,c,d. While the forward part of the angular distributions is reasonably well reproduced, an exceedingly large amount of backward scattering is predicted, possibly due to reflection of the incident wave at the sharp boundary.

Spergel ([11]) used a similar model. He choses the wave number K of each partial wave inside the core in such a way as to maximize the absorption. This results in a strong re

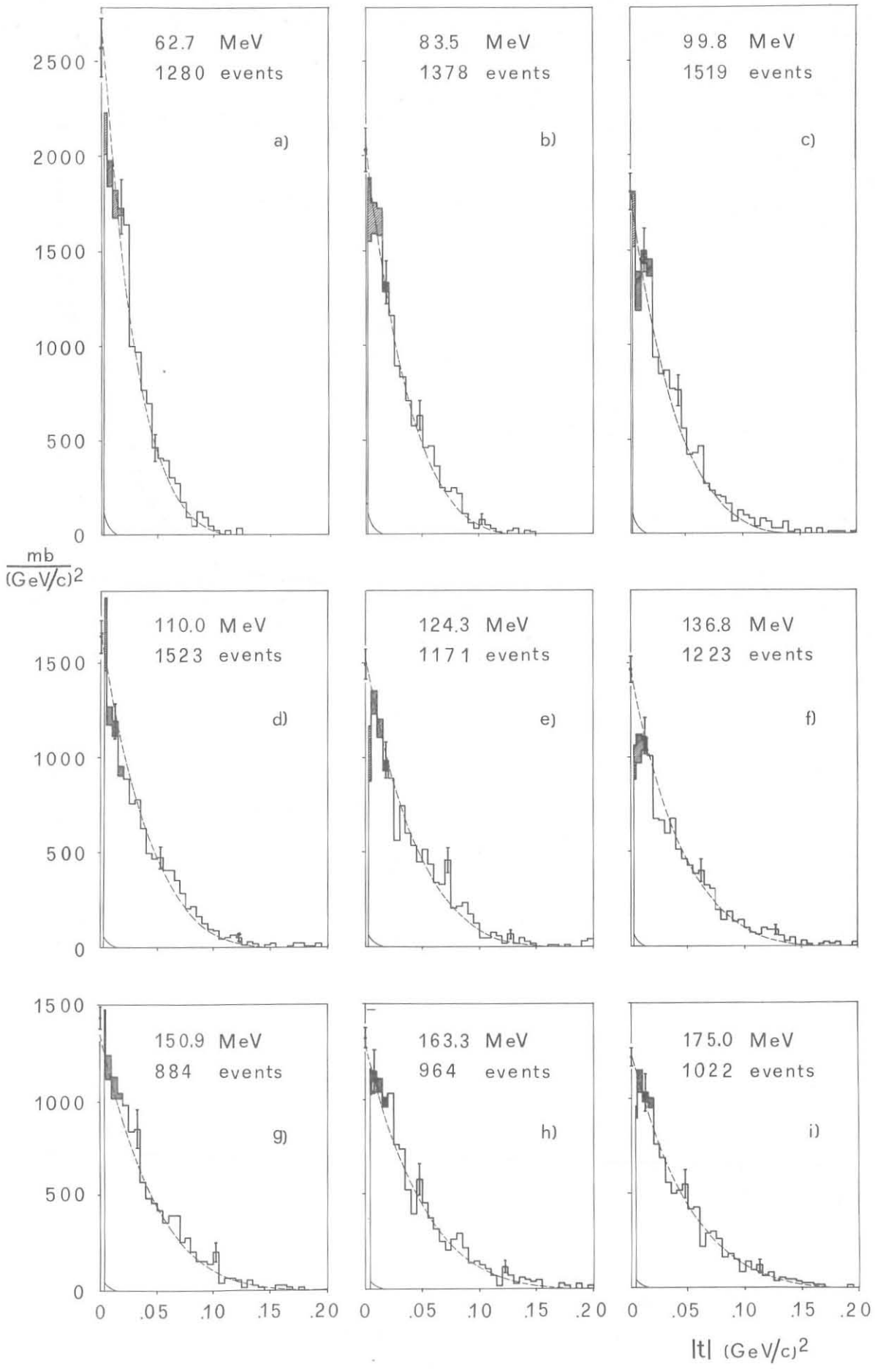

Fig. 3 - Differential cross-sections $d\sigma/dt$ for the 9 energy values for $|t| \leq 0.2$ $(GeV/c)^2$. The full line is the Coulomb differential cross-section which has been subtracted. The solid dot represents the optical point, and the shaded areas the correction due to scattering plane orientation. Typical errors are shown.
The dashed line is the 3 parameters fit of formula (3).

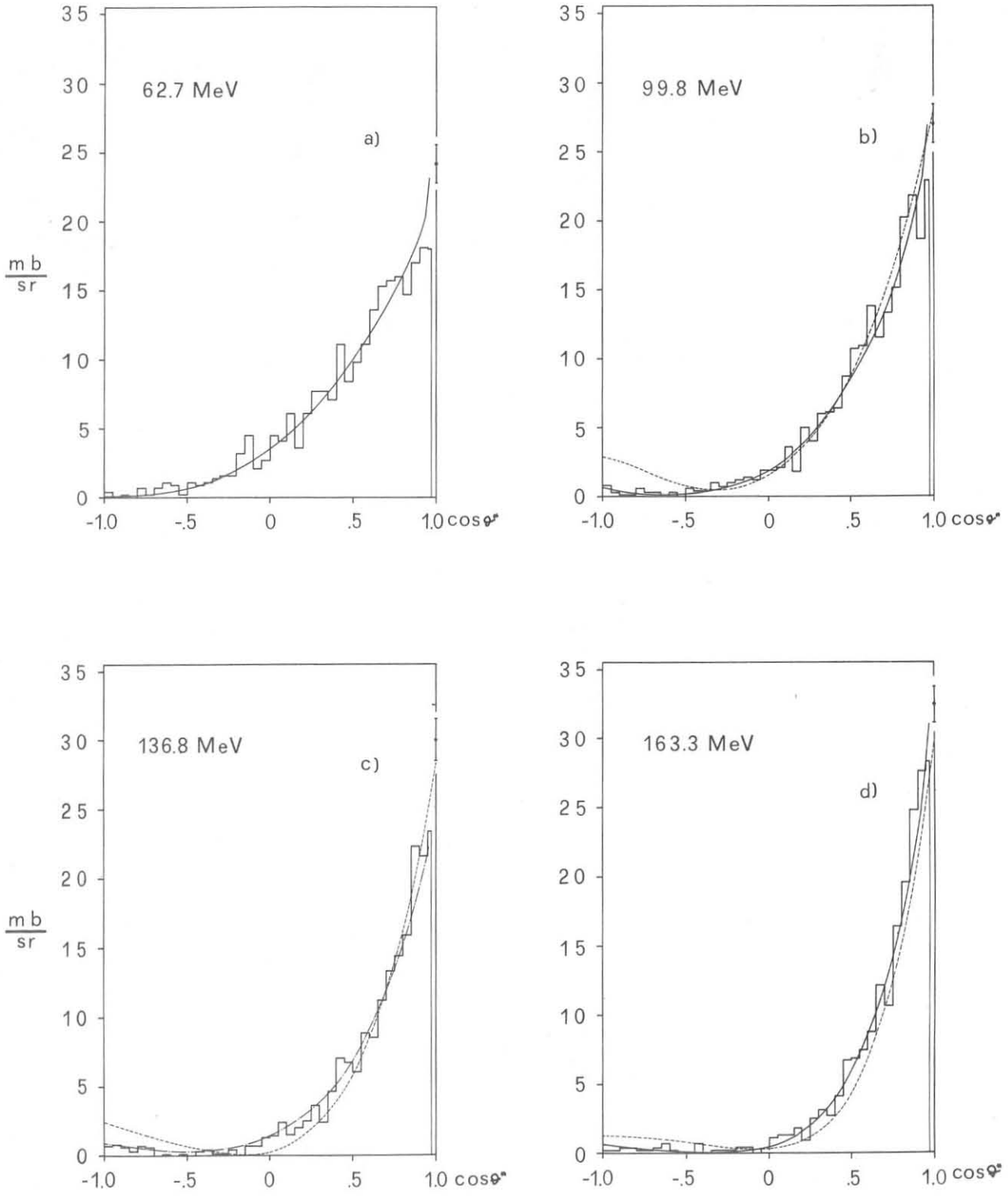

Fig. 4 - Comparison of experimental differential cross-sections $d\sigma/d\Omega$ with theoretical predictions.
Data at 62.7(a), 99.8(b), 136.8(c), 163.3(d) MeV.

Theory ———— Bryan and Phillips at 62.7(a), 99.8(b). 163.3(d) MeV;
– – – – Ceschia and Perlmutter at 96(b), 133(c), 170(d) MeV;
–·–·– Spergel at 140(c) MeV.

TABLE III

T [MeV]	λ [fm]	Optical point [mb/(GeV/c)^2]	$(d\sigma/dt)_{t=0}$ Formula (2)	Formula (3)
62.7	1.149	2569 ± 151	2690	2656
83.5	0.996	2033 ± 112	2120	2095
99.8	0.911	1803 ± 94	1884	1820
110.0	0.867	1644 ± 82	1586	1691
124.3	0.816	1494 ± 79	1454	1544
136.8	0.778	1461 ± 71	1355	1441
150.9	0.740	1433 ± 60	1438	1345
163.3	0.712	1324 ± 53	1335	1274
175.0	0.688	1215 ± 47	1223	1216

duction of the backward scattering. The main difficulty is now that the value of core radius that predicts the correct elastic cross-section gives systematically a much too low annihilation cross-section. As an example in Fig. 4 c, a curve is plotted, corresponding to the choice of the core radius and of the real potential that gives the best value for the total scattering cross-section. There is an improvement of the fit the backward direction but the forward cross-section is now too small.

The introduction of an imaginary potential leaves a large freedom for the choice of its shape. Nemirowskii and Strokov ([12]) have assumed an imaginary potential $V = V_0 \exp(-r/c)$ and a phenomenological description for the real part. With their best choice $V_0 = -4$ GeV; $c = 0.2\,\lambda\!\!\!^{-}_{\pi}$ the elastic cross-section results too low on the average (see I) but there is still with an overestimate of backward events.

The most satisfaction calculations have been made recently by Bryan and Phillips ([13]). They use an imaginary potential of the form $V = V_0/[1+\exp(r/c)]$. The real part was obtained from the Bryan and Scott ([14]) NN potential, this being a sum of one-boson-exchange terms. Since each contribution to the real potential has a definite G parity, the modification to the $\bar{N}N$ case in unambiguous. The two parameters V_0 and c describing the imaginary potential are then fitted to the experimental data. Preliminary results show that an excellent agreement can be obtained both to the total cross-sections and angular distributions with the choice $V_0 = -60$ GeV, c = 1/6 fm.

In Fig. 4a, b, d the predicted differential cross-sections at 62.7, 99.8 and 163.3 MeV are compared with the data.

The energy interval explored by this experiment covers the mass of the S meson ([15]). In terms of the laboratory kinetic energy of the incident antiproton this meson would be formed at 104 ± 28 MeV, with a width of 70 MeV. No significant changes in both the magnitude and shape of the differential cross-section are observed going accross this energy, indicating that this meson does not give rise to any prominent effect in the $\bar{p}p$ elastic channel.

* * *

We would like to thank Prof. B. Gregory and Dr. R. Armenteros for their interest and contributions to the success of the exposure.

We acknowledge the efficient running of the CERN P.S. and of the 81 cm Saclay HBC.

Part of the numerical computations have been performed at the CNAF (Centro Nazionale di Analisi Fotogrammi) at Bologna.

Mr. F. Beccari, Dr. A. Iosi Orlandini and Mr. V. Valente have contributed to the programming work.

We are grateful to Dr. R.J.N. Phillips for advance information about his theoretical results.

* * *

REFERENCES

(1) U. Amaldi jr., B. Conforto, G. Fidecaro, H. Steiner, G. Baroni, R. Bizzarri, P. Guidoni, V. Rossi, G. Brautti, E. Castelli, M. Ceschia, L. Chersovani and M. Sessa: Nuovo Cimento 46, 171 (1966)

(2) C.A. Coombes. B. Cork, W. Galbraith, G.R. Lambertson and W.A. Wenzel: Phys. Rev. 112, 1303 (1958)

(3) B. Cork, O.I. Dahe, D.H. Miller, A.G. Tenner and C.L. Wang: Nuovo Cimento 25, 497 (1962)

(4) H. Hossain and M.A. Shaukat: Nuovo Cimento 38, 737 (1965)

(5) U. Amaldi jr., B. Conforto, G. Fidecaro, H. Steiner, R. Tosi-Torelli, G. Baroni, R. Bizzarri, P. Guidoni, F. Marcelja, V. Rossi, A. Stajano, G. Brautti, E. Castelli, M.Ceschia, L. Chersovani and M. Sessa: Proceedings of the Siena International Conference on Elementary Particles (1963), vol. I, pag. 243

(6) U. Amaldi, T. Fazzini, G. Fidecaro, C. Ghesquière, M. Legros and H. Steiner: Nuovo Cimento 30, 973 (1963)

(7) J.S. Ball and J.F. Chew: Phys. Rev. 109, 1385 (1958)

(8) J.R. Fulco: Phys. Rev. 110, 784 (1958)

(9) J.S. Ball and J.R. Fulco: Phys. Rev. 113, 647 (1959)

(10) M. Ceschia and A. Perlmutter: Nuovo Cimento 33, 578 (1964)

(11) M.S. Spergel: Nuovo Cimento 47, 410 (1967)

(12) P.E. Nemirovskii and Yu. F. Strokov: J. Expth. Theoret. Phys. (U.S.S.R.) 46, 1379 (1964); translated in Soviet Physics JEPT 19, 932 (1964). See also Ju. P. Elagin, P.E. Nemirovskii, Ju. F. Strokov: Phys.Lett.7,352 (1963)

(13) R.A. Bryan and R.J.N. Phillips - Bull. Am. Phys. Soc. 10, 737 (1965) and private communications, see also R.J.N. Phillips: Invited paper at the Gainesville conference on the nucleon-nucleon interaction, March 23-25, (1967)

(14) R.A. Bryan and B.L. Scott: Phys. Rev. 135, B 434 (1964)

(15) G. Chikovani, L. Dubal, M.N. Focacci, W. Kienzle, B. Levrat, B.C. Maglić, M. Martin, C.Nef, P. Schübelin, and J. Séquinot: Phys. Letters 22, 233 (1966). - M.N. Focacci, W. Kienzle, B. Levrat, B.C. Maglić and M. Martin: Phys. Rev. Lett. 17, 890 (1966).

* * *